

# Combined Experimental–Theoretical Characterization of the Hydrido-Cobaloxime [HCo(dmgH)<sub>2</sub>(PnBu<sub>3</sub>)]

Anirban Bhattacharjee,<sup>†</sup> Murielle Chavarot-Kerlidou,<sup>‡</sup> Eugen. S. Andreiadis,<sup>‡</sup> Marc Fontecave,<sup>‡,§</sup> Martin J. Field,<sup>\*,†</sup> and Vincent Artero<sup>\*,‡</sup>

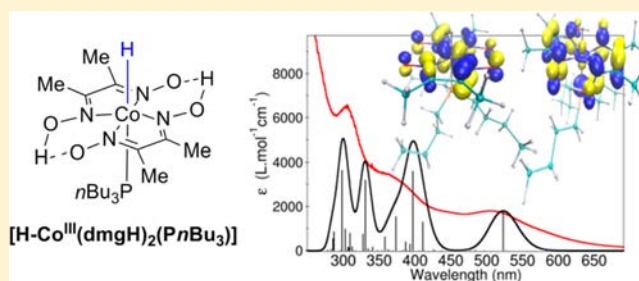
<sup>†</sup>Dynamo Team, DYNAMOP Group, UMR 5075, Université Grenoble 1, CNRS, CEA; Institut de Biologie Structurale “Jean-Pierre Ebel”, 41 rue Jules Horowitz, 38027 Grenoble Cedex 1, France

<sup>‡</sup>Laboratoire de Chimie et Biologie des Métaux, UMR 5249, Université Grenoble 1, CNRS, CEA DSV/iRTSV; CEA-Grenoble, 17 rue des Martyrs F-38054 Grenoble Cedex 9, France

<sup>§</sup>Collège de France, 11 place Marcellin-Berthelot, 75005 Paris, France

## S Supporting Information

**ABSTRACT:** A combined theoretical and experimental approach has been employed to characterize the hydrido-cobaloxime [HCo(dmgH)<sub>2</sub>(PnBu<sub>3</sub>)] compound. This complex was originally investigated by Schrauzer et al. [Schrauzer et al., *J. Am. Chem. Soc.* **1971**, *93*,1505] and has since been referred to as a key, stable analogue of the hydride intermediate involved in hydrogen evolution catalyzed by cobaloxime compounds [Artero, V. et al. *Angew. Chem., Int. Ed.* **2011**, *50*, 7238–7266]. We employed quantum chemical calculations, using density functional theory and correlated RI-SCS-MP2 methods, to characterize the structural and electronic properties of the compound and observed important differences between the calculated <sup>1</sup>H NMR spectrum and that reported in the original study by Schrauzer and Holland. To calibrate the theoretical model, the stable hydrido tetraamine cobalt(III) complex [HCo(tmen)<sub>2</sub>(OH<sub>2</sub>)<sub>2</sub>]<sup>2+</sup> (tmen = 2,3-dimethyl-butane-2,3-diamine) [Rahman, A. F. M. M. et al. *Chem. Commun.* **2003**, 2748–2749] was subjected to a similar analysis, and, in this case, the calculated results agreed well with those obtained experimentally. As a follow-up to the computational work, the title hydrido-cobaloxime compound was synthesized and recharacterized experimentally, together with the Co(I) derivative, giving results that were in agreement with the theoretical predictions.



## INTRODUCTION

Cobaloxime compounds<sup>1,2</sup> and related diimine-dioxime compounds<sup>3</sup> have emerged in the past few years as one of the most efficient series of molecular catalysts for hydrogen evolution, and a significant number of studies have been performed to understand the mechanisms of their electro- and photocatalytic activities.<sup>3–15</sup> It is generally well-accepted that the catalytic cycle for hydrogen evolution passes through a hydrido-cobaloxime intermediate<sup>1</sup> obtained through protonation of a Co(I) species, as formation and cleavage of the Co–H bond is found to play a crucial role in catalysis. Recent independent reports from Muckerman and Hammes-Schiffer have addressed such mechanistic issues using theoretical chemistry methods.<sup>16,17</sup>

Up until now, the only study so far dedicated to the isolation of this crucial intermediate is one by Schrauzer and Holland that dates back to 1971.<sup>18</sup> However, the spectroscopic characterizations in that paper raise questions about the exact nature of the compound that was present.<sup>18,19</sup> Specifically, in their reported <sup>1</sup>H NMR spectrum, a chemical shift at +6.0 ppm was claimed to be the signature of the hydrogen atom bound to

the cobalt center (cobalt-bound hydrogen, hereafter abbreviated as CBH).<sup>1,18</sup> Although not unprecedented among transition metal hydrides,<sup>20–22</sup> this value is surprising for a formal hydride ligand which is generally characterized by a negative <sup>1</sup>H NMR chemical shift.<sup>23–25</sup> An example may be found in the relatively recent study of another Co(III) CBH compound, the hydrido tetraamine cobalt(III) complex [HCo(tmen)<sub>2</sub>(OH<sub>2</sub>)<sub>2</sub>]<sup>2+</sup> (**1**).<sup>26</sup> Another issue is the characteristic blue color of such hydrido-cobaloxime compounds that is associated with a strong absorption in the 500–600 nm range,<sup>18,27</sup> in sharp contrast with the yellow color reported for [HCo(tmen)<sub>2</sub>(OH<sub>2</sub>)<sub>2</sub>]<sup>2+</sup><sup>26</sup> and other Co(III) derivatives in the cobaloxime series.

Because of the importance of this compound for the elucidation of H<sub>2</sub>-evolving cobalt-based mechanisms, we have undertaken a new characterization of the title hydride complex [HCo(dmgH)<sub>2</sub>(PnBu<sub>3</sub>)] (**2**) using both experimental and theoretical approaches. We aimed to confirm the hydridic

Received: November 10, 2011

Published: June 19, 2012

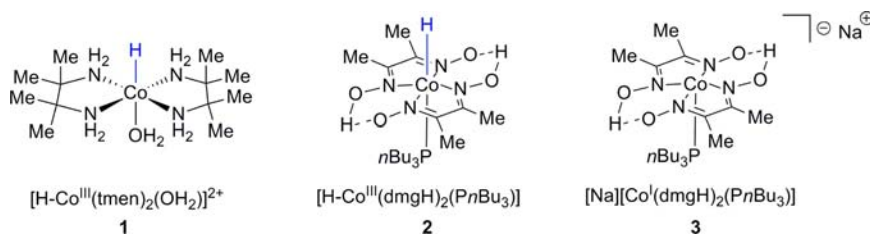


**Figure 1.** Schematic representations of the complexes  $[\text{HCo}(\text{tmen})_2(\text{OH}_2)]^{2+}$  (1),  $[\text{HCo}(\text{dmgH})_2(\text{PnBu}_3)]$  (2), and  $[\text{Na}][\text{Co}(\text{dmgH})_2(\text{PnBu}_3)]$  (3).

nature of CBH in 2 and also to provide a more detailed insight into the structural and electronic properties of 2. In this paper, we first present the results of calculations regarding the recently characterized hydridotetraamine cobalt(III) compound 1,<sup>26</sup> as a way of calibrating our theoretical model, before describing the ground and excited state properties of the target hydrido-cobaloxime derivative 2. Characterization of the Co(I) complex  $[\text{Co}(\text{dmgH})_2(\text{PnBu}_3)]^-$  (3) is also provided. Structures of all three complexes are presented in Figure 1.

## MATERIALS AND METHODS

**Materials and Instrumentation.** The complexes  $[\text{Co}^{\text{III}}(\text{dmgH})_2(\text{pyr})\text{Cl}]^{28}$  and  $[\text{Co}^{\text{III}}(\text{dmgH})_2(\text{PnBu}_3)\text{Cl}]^{29}$  were prepared according to previously reported literature procedures. Dimethylglyoxime (dmgH<sub>2</sub>), pyridine, cobalt chloride hexahydrate, *n*-tributylphosphine, sodium borohydride, sodium phosphate monobasic, and sodium phosphate dibasic were used as received. Spectroscopic grade acetonitrile and toluene were thoroughly degassed before use for the UV–visible absorption studies. Deuterated acetonitrile was purchased from Euriso-top and stored in the glovebox.

<sup>1</sup>H NMR spectra were recorded at room temperature in 5 mm o.d. tubes on a 300 MHz Bruker AC300 spectrometer equipped with a QNP probehead. UV–visible absorption spectra were recorded on a Shimadzu UV-1800 spectrophotometer. FTIR spectra were recorded with a Perkin-Elmer Spectrum-100 spectrophotometer equipped with a Pike Miracle ATR accessory (Ge crystal).

**[HCo(dmgH)<sub>2</sub>(PnBu<sub>3</sub>)](2).** The synthesis of the hydride complex was adapted from the procedure described by Schrauzer and Holland.<sup>18</sup> A buffered aqueous solution was prepared as follows: 4.5 mmol (351 mg) of NaH<sub>2</sub>PO<sub>4</sub> and 4.5 mmol (401 mg) of Na<sub>2</sub>HPO<sub>4</sub> were dissolved in 25 mL of H<sub>2</sub>O. The pH was measured and found to be ~7. Then, 25 mL of MeOH were added, and the pH was readjusted to ~7 by addition of NaH<sub>2</sub>PO<sub>4</sub>. In a glovebox, 0.2 mmol (99 mg) of cobaloxime  $[\text{Co}^{\text{III}}(\text{dmgH})_2(\text{PnBu}_3)\text{Cl}]$  were suspended in 5 mL of the above solution and equilibrated for 1 night under N<sub>2</sub>. An aqueous solution of NaBH<sub>4</sub> (32 mg in 0.5 mL H<sub>2</sub>O) was added dropwise to the suspension. The resulting foaming mixture was stirred for 0.5 h before being filtered under vacuum. A purple dark solid was collected, washed with water until the filtrate was colorless, and dried under vacuum. Samples for <sup>1</sup>H NMR, mass spectrometry, UV–visible and IR spectroscopic measurements, and elemental analysis were prepared in the glovebox.

<sup>1</sup>H NMR (300 MHz, CD<sub>3</sub>CN):  $\delta$  in ppm 16.05 (s, 2H, dmgH), 2.32, 2.20, 2.19, 2.13 (s, 12H, CH<sub>3</sub><sup>dmg</sup>), 1.30 (m, 18H, CH<sub>2</sub><sup>Bu</sup>), 0.88 (bd t, 9H, CH<sub>3</sub><sup>Bu</sup>), –5.06 (bs, 1H, H–Co).

MS (ESI, MeOH):  $m/z$  = 491 ( $[\text{M} - \text{H}]^+$ ); 289 ( $[\text{M} - \text{H} - \text{P}(\text{nBu}_3)]^+$ ).

Elemental analysis: Calcd for 3·0.4 Na<sub>3</sub>PO<sub>4</sub>: C, 43.05; H, 7.59; N, 10.04. Found: C, 42.74; H, 7.40; N, 9.72.

UV–vis in CH<sub>3</sub>CN:  $\lambda_{\text{max}}$  in nm ( $\epsilon$  in L mol<sup>–1</sup> cm<sup>–1</sup>) 506 (1800), 365 (shoulder, 3442), 305 (6726). UV–vis in cyclohexane: 567 (3398), 380 (2344), 309 (4409).

FTIR-ATR: 2957, 2928, 2870, 1543, 1456, 1377, 1227, 1088, 975, 907, 777, 723 cm<sup>–1</sup>.

**[Na][Co<sup>I</sup>(dmgH)<sub>2</sub>(PnBu<sub>3</sub>)](3).** The preparation of the reduced Co(I) cobaloxime was adapted from a reported procedure.<sup>30,31</sup>  $[\text{Co}^{\text{III}}(\text{dmgH})_2(\text{PnBu}_3)\text{Cl}]$  (120 mg, 0.23 mmol) was dissolved in

distilled methanol (6 mL) in a Schlenk flask under Ar. A degassed NaOH solution in distilled methanol (1.5 mL, 1N) was added, and then NaBH<sub>4</sub> (85 mg, 2.3 mmol) was introduced as solid. The resulting dark-blue suspension was vigorously stirred for 10 min, and the solvent was evaporated to dryness. Distilled acetonitrile (10 mL) was added to solubilize the Co(I) complex, and the solution was rapidly filtered via cannula. The solvent was evaporated to dryness to give 110 mg of a dark-blue powder consisting of  $[\text{Na}][\text{Co}^{\text{I}}(\text{dmgH})_2(\text{PnBu}_3)]$  together with residual NaBH<sub>4</sub> (7 equiv/Co as determined by <sup>1</sup>H NMR).

<sup>1</sup>H NMR (300 MHz, CD<sub>3</sub>CN):  $\delta$  in ppm 19.11 (s, 2H, dmgH), 2.33–2.09 (m, 12H, CH<sub>3</sub><sup>dmg</sup>), 1.24–1.12 (m, 18H, CH<sub>2</sub><sup>Bu</sup>), 0.85 (t, 9H, CH<sub>3</sub><sup>Bu</sup>).

UV–vis in MeOH:  $\lambda_{\text{max}}$  in nm ( $\epsilon$  in L mol<sup>–1</sup> cm<sup>–1</sup>) 614 (4090), 400, 305 (shoulder).

**Theoretical Calculations.** Calculations were performed using the ORCA quantum chemical program<sup>32</sup> at the density functional theory (DFT) and second-order Møller–Plesset perturbation theory (MP2) levels of theory. For the DFT calculations, we employed the popular B3LYP hybrid functional<sup>33,34</sup> and also the BP86 GGA functional,<sup>35,36</sup> as the latter has been shown to provide more precise results than B3LYP for the cobalt corrinoids,<sup>37,38</sup> to which the cobaloxime complexes stand as functional models. The MP2 calculations were done with the improved “spin component scaling” framework<sup>39</sup> and the resolution of identity approximation (RI-SCS-MP2). Although we will concentrate on the DFT results, the RI-SCS-MP2 values are included as the MP2 method is one of the few wave function-based methods that takes some account of electron correlation and is applicable to transition metal systems of the size we are studying. We used the Ahlrichs triple zeta valence plus polarization (TZVP) basis,<sup>40</sup> which is of triple- $\zeta$  quality, for both the DFT and MP2 calculations. Although the DFT results are not overly dependent on the basis, a higher quality basis is preferable when using MP2.

All structures were fully geometry optimized, in solvent, at the relevant levels of theory using tight convergence criteria. The effect of solvent was included in all DFT and MP2 geometry optimizations and property calculations via the COSMO implicit solvation model that is implemented in ORCA.<sup>41</sup>

Charge population analyses were carried out on the optimized structures using electrostatic potential (ESP), Löwdin and Mulliken population analyses.<sup>42,43</sup> The absolute values of the atomic charges obtained from these models can vary quite substantially, although the ESP values are often regarded to be the most reasonable, at least for small molecules. We note, however, that even though the absolute values may not be reliable, the trends in the values between the different methods are often well reproduced.

NMR <sup>1</sup>H chemical shifts were calculated using the individual gauge of localized orbitals (IGLO) method,<sup>44</sup> implemented in ORCA,<sup>32</sup> for the DFT geometry-optimized structures only. In addition to the TZVP basis we also employed the IGLO-III basis that has been optimized for these types of calculation.<sup>45</sup> Chemical shift values are reported with respect to those of a TMS reference, geometry optimized in solvent with the same level of theory and basis set.

For the calculation of the UV–visible spectra of the compounds we employed the time-dependent DFT (TDDFT) method in the appropriate solvent. Given the variable nature of the results that can be obtained with TDDFT, we tried a number of functionals, in addition to BP86 and B3LYP, and also the smaller 6-31G(d,p) basis as well as TZVP. We fit the spectra using the standard method with fwhm

values of 3500, 1675, and 992  $\text{cm}^{-1}$  to reproduce the extinction coefficient values corresponding to the experimentally observed energy transitions of **1** in water and **2** in  $\text{CH}_3\text{CN}$  and cyclohexane respectively.

## RESULTS AND DISCUSSION

**[HCo(tmen)<sub>2</sub>(OH<sub>2</sub>)<sup>2+</sup> (1).** This moderately stable cobalt(III)-hydride compound was described in 2003 and characterized in water. The crystal structure from the reported X-ray diffraction study<sup>26</sup> was used as the starting point for our calculations. Initially, hydrogen atoms were added and their positions geometry optimized using DFT calculations. After this, full geometry optimizations were performed with an implicit water solvation model, to give the structural information appearing in Table 1 and Supporting Information,

**Table 1. Comparison of Geometrical Parameters Obtained from Experiment and DFT Calculations for [HCo(tmen)<sub>2</sub>(OH<sub>2</sub>)<sup>2+</sup> 1**

parameter	experimental	DFT/BP86	DFT/B3LYP	RI-SCS-MP2
Distances (Å)				
Co–N	1.95	1.96	1.97	1.96
Co–O	2.10	2.12	2.15	2.15
Co–H		1.44	1.43	1.37
C–C(eq)	1.51	1.58	1.57	1.55
Angles (degrees)				
N–Co–N	82, 86	84	83	84.5
N–Co–H		88	88	88

Table S1 and in Figure 2. In these calculations, the axial water ligand present in the experimental crystal structure was explicitly included to satisfy the metal's coordination requirement.

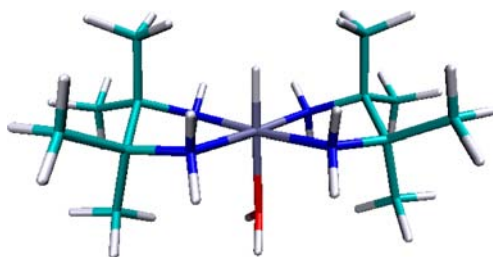


**Figure 2.** Structure of the hydrido tetraamine cobalt(III) [HCo(tmen)<sub>2</sub>(OH<sub>2</sub>)<sup>2+</sup> (**1**)] optimized in water with the BP86 functional and the TZVP basis set.

The BP86 and B3LYP functionals produce very similar geometries with the given TZVP basis, although the coordination sphere geometry (Co–N and axial Co–O distances) is closest to experiment for BP86. Both B3LYP and RI-SCS-MP2 produce slightly elongated axial Co–O bonds. The most marked difference between the DFT and RI-SCS-MP2 methods is seen for the axial Co–H distance which is much shorter for the latter than the former (1.37 Å as opposed to 1.43–1.44 Å).

An ESP charge population analysis of the geometry optimized structures gives the following ordering for the populations of the different types of hydrogen present in the molecule, H(Co) < H(C-Alkyl) < H(N) < H(O), with values of 0.02, 0.05, 0.21, and 0.25, respectively. The latter should mirror the electronic shielding undergone by the different

hydrogen nuclei and this is indeed so, as the calculated and experimental (in parentheses) chemical shift values, in ppm, with respect to TMS are –10 (–23), 1–2 (1.1), 2.6–3.2 (2.8), and 3.0 (3.3) ppm for H(Co)/CBH, H(C–Alkyl), H(N), and H(O), respectively. The value at –10 ppm exhibits variations of the order of ~4 ppm when different basis sets (IGLO-III, TZVP) and functionals (B3LYP and BP86) are used, whereas the others vary only by 0.1–0.3 ppm. The chemical shifts for the downfield protons are in good agreement with experiment, but the value for the CBH differs by 7.0 ppm from the experimental value. Nevertheless, its high diamagnetic deshielding behavior, which is characteristic of transition metal hydrides, is clearly evident. We note, however, that similar differences between the calculated and experimental shifts of metal-bound hydrides have been observed in a recent comprehensive study of transition metal hydrides.<sup>41</sup> Experimentally, compound **1** has absorption maxima,  $\lambda_1$  and  $\lambda_2$ , in its UV–vis absorption spectrum at 444 and 340 nm, respectively. The TDDFT calculated values are displayed in Table 2 and

**Table 2. Comparison of the UV-VIS Absorption Spectra from Experiment<sup>26</sup> and DFT Calculations for 1 Using Different Functionals and the TZVP and 6-31G(d,p) Basis Sets**

method	$\lambda_1/\text{nm}$	$\lambda_2/\text{nm}$
<b>Experiment</b>	444	340
<b>GGA functionals/TZVP basis</b>		
BP86	400	337
PBE	400	338
<b>Hybrid functionals/TZVP basis</b>		
B3LYP	415	326
PBE0	428	332
<b>GGA functionals/6-31G(d,p) basis</b>		
BP86	430	354
PBE	434	360
PWLDA	450	375
<b>Hybrid functionals/6-31G(d,p) basis</b>		
B3LYP	439	336
PBE0	455	374

Supporting Information, Figure S7, which shows that all functionals and both basis sets give results that are in reasonable agreement with experiment. The disagreement is most pronounced for the  $\lambda_1$  peak with the GGA functionals and the TZVP basis, although this is corrected by going to the smaller 6-31G(d,p) basis. Population analysis indicates that the orbitals involved in the transitions are predominantly of “d–d” type, although the upper states have considerable  $\sigma$  antibonding character, centered on the metal. More details may be found in Supporting Information, Tables S2 and S3.

To conclude this section, we note that the DFT approaches that we employ are capable of reproducing the crystal structure and the hydride nature of the CBH of compound **1** in a robust fashion. It also enables the UV–visible spectrum to be determined, although these calculations are more sensitive to the combination of functional and basis set that are used. It is true that compound **2** has some significant chemical differences to compound **1**, but these preliminary calculations nevertheless provide an idea of the accuracy that can be attained when studying CBH species.

**[HCo(dmgh)<sub>2</sub>(PnBu<sub>3</sub>)] (2).** To our knowledge, no X-ray crystallographic structure has been reported for the hydride

compound **2**. The closest available structure to which it can be compared is that of the *trans*-chlorobis(dimethylglyoximate)-(tri-*n*-butylphosphine)cobalt(III) complex.<sup>46</sup> As a result, the starting structure for the geometry optimization of the hydride complex was obtained by model building from the crystallographic data of this cobalt(III) compound.<sup>46</sup>

Structural parameters obtained after geometry optimization in an implicit solvent model of acetonitrile are summarized in Table 3 and Supporting Information, Table S4 for different

**Table 3. Summary of Geometrical Parameters Obtained from Theoretical Geometry Optimizations of [HCo(dmgH)<sub>2</sub>(P*n*Bu<sub>3</sub>)] **2** Using the TZVP Basis Set**

parameter	BP86	B3LYP	RI-SCS-MP2
Distances (Å)			
Co–H	1.49	1.47	1.41
Co–N	1.89,1.90	1.91,1.92	1.88,1.89
N–O	1.33,1.37	1.31,1.37	1.32,1.37
O–H	1.09	1.04	1.04
O...H	1.40	1.52	1.48
O...O	2.49	2.54	2.51
C–C(sp <sup>2</sup> )	1.46	1.46	1.46
Co–P	2.34	2.42	2.33
C(sp <sup>3</sup> )-C(sp <sup>2</sup> )	1.49	1.49	1.5
C(sp <sup>3</sup> )-C(sp <sup>3</sup> )	1.54	1.54	1.53
C–N	1.32,1.30	1.31,1.30	1.32,1.30
Angles (degrees)			
N–Co–N (out of plane)	169,172	170,174	170,175
H–Co–N	87,85	87,85	87,85
O...H–O	171	168	169
H–Co–P	179	179	178

levels of theory, and an optimized structure is presented in Figure 3. The BP86, B3LYP, and RI–SCS–MP2 methods

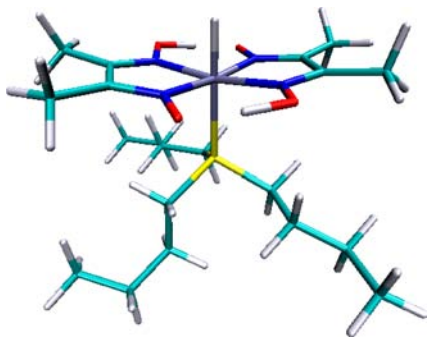


**Figure 3.** Structure of hydrido-cobaloxime [HCo(dmgH)<sub>2</sub>(P*n*Bu<sub>3</sub>)] (**2**) optimized in acetonitrile with the BP86 functional and the TZVP basis set.

generally agree well among themselves, except for the axial Co–P and Co–H bond distances, and the structure of the H-bridges. The axial Co–P (2.34 Å) bond distance produced by BP86 closely resembles that of RI–SCS–MP2 (2.33 Å), whereas the Co–H bond distance obtained with RI–SCS–MP2 (1.41 Å) is considerably shorter than those obtained with both B3LYP (1.47 Å) and BP86 (1.49 Å). Overall the coordination structure is octahedral, although with slight distortions, as the Co atom lies above the plane of the four N atoms of the cobaloxime ligands (the N–Co–N angles are

169–173° instead of 180°) in the direction of the phosphorus atom.

Bond lengths from the reference structure of the *trans*-chlorobis(dimethylglyoximate)(tri-*n*-butylphosphine)cobalt(III) complex,<sup>46</sup> such as Co–N (1.88–1.89 Å), N–O (1.33–1.37 Å), equatorial planar C–C (1.44–1.48 Å) and C–N (1.28–1.32 Å), are in good agreement with those we calculate for **2**. The Co–P distances are, however, not comparable since the *trans* ligands are different. A slightly longer Co–P distance is expected and indeed observed (2.33–2.6 Å) for **2** given the stronger structural *trans* effect of the hydride ligand, compared to that of the chloride ligand (Co–P bond length in the reference Co(III) compound: 2.27 Å).<sup>47</sup> In addition, the hydride compound **2** displays a similar out of plane shift of the Co atom toward the P atom.

The results of Mulliken and ESP charge population analyses for the optimized geometries of **2** are summarized in Table 4.

**Table 4. Mulliken and ESP Atomic Charges at the Optimized Geometries of [HCo(dmgH)<sub>2</sub>(P*n*Bu<sub>3</sub>)] **2**<sup>a</sup>**

atom	method		
	BP86	B3LYP	RI-SCS-MP2
Co	–0.02, –0.77	–0.21, –0.71	–0.30, –0.34
H(Co–H)	0.04, –0.04	–0.00, –0.07	0.09, –0.19
H(O–H)	0.28, 0.47	0.29, 0.49	0.27, 0.55
O(Protonated)	–0.26, –0.54	–0.29, –0.58	–0.30, –0.65
O(Deprotonated)	–0.37, –0.57	–0.45, –0.62	–0.49, –0.75
H(Methyl)	0.13, 0.10	0.12, 0.09	0.11, 0.10

<sup>a</sup>Mulliken charges occur first in each entry.

As is well-known, the Mulliken and ESP values differ, yet some trends are evident. The DFT and RI–SCS–MP2 charges differ for Co and CBH but are otherwise quite similar. The DFT ESP charges for the oxygen atoms in the H-bridges are almost the same, which is indicative of a strong hydrogen bond between them. Likewise, the DFT ESP charges for the CBH are only slightly negative, whereas the RI–SCS–MP2 value reflects a clearer hydridic nature. The Co–H bond itself is highly covalent as its Mayer bond orders are 0.79, 0.90, and 0.86 with the BP86, B3LYP, and RI–SCS–MP2 methods, respectively.

We calculated the <sup>1</sup>H NMR chemical shifts using the BP86 functional and the TZVP and IGLO-III basis sets, which gave shifts for the CBH of –4 and –6.5 ppm, respectively. Given the similarities in the two sets of results, we concentrate on the IGLO-III values in what follows. The O–H protons show high downfield shifts of 18.5 ppm, whereas the shifts of the methyl protons from the dmgH<sup>–</sup> ligand are slightly upfield (2.1–2.4 ppm) compared to the *n*-butyl protons of the phosphine ligand (0.9–1.5 ppm). The RI–SCS–MP2 optimized geometry with a shorter Co–H bond length yields a slightly more negative value of –6.8 ppm. Overall these values agree with the negative values that are most often reported for transition metal hydrides,<sup>23–25</sup> but contrast strongly with the +6 ppm value reported by Schrauzer et al.<sup>18</sup>

As a result of these calculations, we decided to study the hydride complex **2** experimentally. It was synthesized by NaBH<sub>4</sub> reduction of the Co(III) complex [Co(dmgH)<sub>2</sub>(P*n*Bu<sub>3</sub>)Cl]<sup>29</sup> in a phosphate-buffered aqueous methanolic solution.<sup>18</sup> A purple solid was obtained as described in Schrauzer's procedure but dried under vacuum at room temperature. When analyzed by <sup>1</sup>H NMR in CD<sub>3</sub>CN (Supporting Information, Figure S1), the isolated purple dark

powder displays one singlet signal at  $-5.06$  ppm, integrating to one proton, together with signals characteristic of the cobalt-coordinated tri-*n*-butylphosphine and the dimethylglyoximate ligands. It should be highlighted that no signal was observed between 3 and 10 ppm, in contrast with Schrauzer's description of the Co-coordinated hydride. A similar spectrum is obtained in cyclohexane ( $\delta(\text{Co-H}) = -6.40$  ppm) when used as a user-friendly surrogate for *n*-hexane to get closer to the conditions used by Schrauzer in 1971. The hydride ligand is not exchanged with  $\text{D}^+$  when a cyclohexane solution of **2** is added with  $\text{D}_2\text{O}$ . The signal at  $-5.06$  ppm slowly disappears when the solution is exposed to air (Supporting Information, Figure S1).

To conclude from the above experimental characterization, it appears that the procedure reported by Schrauzer actually yields a cobalt-hydride compound with a classical high field signal in the  $^1\text{H}$  NMR spectrum.

The FTIR-ATR spectrum of the purple compound does not show any obvious stretching band between 2300 and 1800  $\text{cm}^{-1}$  (Supporting Information, Figure S4). This contrasts with Schrauzer's observation of a band at 2240  $\text{cm}^{-1}$ , but we note that Co-H stretching frequencies for cobalt hydride complexes containing ancillary phosphine ligands typically lie within a range of 1760–1964  $\text{cm}^{-1}$ .<sup>48,49</sup> In the case of **2** there is probably a strong mixing of the Co-H stretching mode with other normal vibration modes of the  $\text{dmgH}^-$  ligands that prevents a straightforward assignment.

A remarkable feature of **2** is its purple color which contrasts both with the orange-brownish color of other Co(III) derivatives in the cobaloxime series and with the yellow color of **1**. Formally **2** and  $[\text{ClCo}(\text{dmgH})_2(\text{P}n\text{Bu}_3)]$  are both Co(III) complexes. Except from the axial ligand, these two complexes have the same composition and geometric structure but their distinct colors indicate a very different electronic structure. A first insight into the difference between chloride and hydride as ligand can be gained from point charge calculations. Both Mulliken and ESP methods show that the chloride ligand bears a net negative charge (BP86/Mulliken:  $-0.36$ ; BP86/ESP:  $-0.48$ ) while the cobalt-hydride bond appears much more covalent with approximately no net charge on the hydrogen atom (Table 4). This clearly indicates that the formal +III oxidation state in **2** is not likely to be in good agreement with its spectroscopy.

The UV-visible spectrum of our sample has been recorded in  $\text{CH}_3\text{CN}$  (Figure 4) and cyclohexane (Supporting Information, Figure S5). They display a broad absorption band responsible for their purple color that shifts from 506 nm ( $\epsilon =$

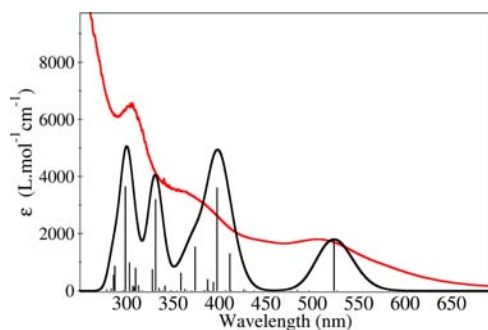


**Figure 4.** UV-visible spectrum of  $[\text{HCo}(\text{dmgH})_2(\text{P}n\text{Bu}_3)]$  in acetonitrile obtained from the experiment (present work) along with the calculated TDDFT transitions (BP86 functional and the TZVP basis set) shown as vertical lines.

1800  $\text{mol}^{-1} \text{L cm}^{-1}$ ) in  $\text{CH}_3\text{CN}$  to 567 nm ( $\epsilon = 3398 \text{ mol}^{-1} \text{L cm}^{-1}$ ) in cyclohexane because of the decreasing polarity of the medium. The  $\lambda_{\text{max}}$  value measured in cyclohexane is similar to that reported by Schrauzer et al. in *n*-hexane.

In a back and forth interplay between theory and experiment we investigated in more detail the electronic absorption spectroscopic features using computational methods. TDDFT calculations for the hydrido-cobaloxime were carried out in acetonitrile with the B3LYP and BP86 functionals and the TZVP and 6-31G(d,p) basis sets. We first concentrate on the results with the BP86 functional and the TZVP basis set. A comparison of the calculated and experimental spectra is shown in Figure 4. Additional analyses are given in Figure 5 and Supporting Information, Tables S5 to S8. Within a comparable orbital energy window, ranging from 400 to 700 nm, the absorptions calculated using BP86/TZVP are found at 397, 411, and 523 nm with the latter value being close to the experimental absorption maximum in that region ( $\lambda_{\text{max}} = 506$  nm in  $\text{CH}_3\text{CN}$ ). For comparison, BP86/6-31G(d,p) calculations yield absorptions at 401, 414, and 546 nm. Using cyclohexane as the implicit solvent, TDDFT could reproduce the experimentally observed bathochromic shift although with a lower magnitude (Supporting Information, Figure S8). An analysis of the orbitals involved in the transition (Figure 5 and Supporting Information, Tables S5 to S8) indicates that this absorption arises principally from HOMO-LUMO (90%) charge transfer with a minor contribution from HOMO-1 to LUMO+1. Population analysis shows the HOMO to be a delocalized orbital with 50% "d" character whereas the LUMO is a delocalized,  $\pi$ -character antibonding orbital, mostly from the ligands. In  $[\text{HCo}(\text{tmen})_2(\text{OH}_2)]^{2+}$  the absence of low-lying conjugated  $\pi^*$  orbitals in the tmen ligand suppresses the absorption in the 500–600 nm region and explains why  $[\text{HCo}(\text{tmen})_2(\text{OH}_2)]^{2+}$  is yellow in color, in contrast to the bluish-purple of  $[\text{HCo}(\text{dmgH})_2(\text{P}n\text{Bu}_3)]$ .

Unlike compound **1**, we note that there is a marked difference when the B3LYP functional is employed for **2**. The higher wavelength band (520–540 nm) is completely missing. The lower transition, at 418 nm with the TZVP basis, is of mixed character, with contributions both from "d-d" and CT-type excitations (Figure 5 and Supporting Information, Tables S5 to S8). We note that Fujita and Muckerman also calculate a single absorption band near 400 nm for the analogous  $[\text{Co}^{\text{III}}\text{H}(\text{dmgBF}_2)_2(\text{CH}_3\text{CN})]$  complex using TDDFT and the B3LYP functional.<sup>16</sup> This apparent inconsistency of the B3LYP and BP86 functionals is perhaps surprising, although a few recent studies have highlighted this particular problem. Noteworthy is a very recent benchmarking study by Kozłowski et al. which deals with excited state calculations of the cobalt-containing vitamin B12.<sup>37</sup> Use of LC-B3LYP, instead of B3LYP, as discussed in ref 37 did not give better agreement with the experimental data. We note that the equal metal and ligand contribution in the HOMO composition of **2** indicates that the bisglyoximate pseudomacrocyclic behaves as a redox-active (noninnocent) ligand which prevents an unequivocal determination of the  $d^n$  electron configuration at the metal ion and the assignment of a definitive Co(III) spectroscopic oxidation state.<sup>50</sup>

Similar features have been observed by others for cobalt trisglyoximate complexes, though at the Co(I) state. Thus, for example, calculations with sophisticated correlated ab initio methods estimated at 28% the contribution of the reduction of the glyoxime ligand to the electronic ground state.<sup>51</sup>

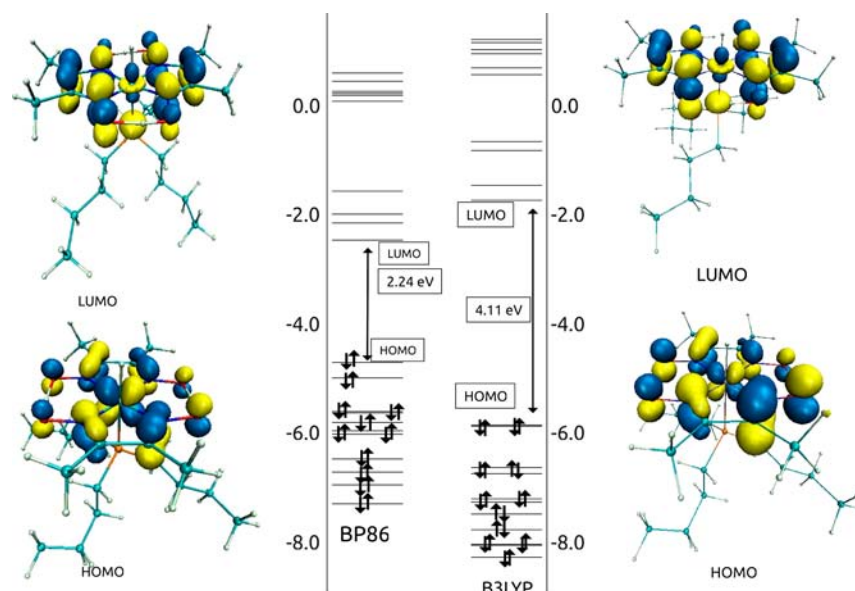


**Figure 5.** Molecular orbital diagrams calculated for **2** with BP86 and B3LYP functionals and representation of the molecular orbitals involved in the transition which is responsible for the intense bluish-purple color of the complex.

Computations of this type are out of the scope of the current study, but would be interesting in the future to probe in further detail the electronic ground state of the hydride. Nevertheless, our simulations of both the  $^1\text{H}$  NMR and UV–visible spectra allow us to confirm that the synthesized compound corresponds to the  $[\text{HCo}(\text{dmgH})_2(\text{PnBu}_3)]$  complex.

We also prepared the cobalt(I) compound  $[\text{Na}][\text{Co}(\text{dmgH})_2(\text{PnBu}_3)]$  (**3**) following a procedure similar to that used for the preparation of **2**, but carried out under alkaline conditions instead of in a buffered pH 7 solution.<sup>31</sup> Crude samples of **3**, containing  $\text{NaBH}_4$  (estimated to 7 equiv/Co by  $^1\text{H}$  NMR) were used for spectroscopic characterization since the excess of reducing agent prevented reoxidation of this air-sensitive compound. The  $^1\text{H}$  NMR spectrum (Supporting Information, Figure S3) indicates the diamagnetic nature of **3**. No signal is observed between 3 and 10 ppm, nor in the high field region where a signal would be expected for a hydride ligand. The UV–visible spectrum of **3** in  $\text{CH}_3\text{OH}$  displays a strong absorption band at 610 nm (Supporting Information, Figure S6), in close agreement with the spectrum previously described for this compound in the same solvent.<sup>19</sup> The  $\lambda_{\text{max}}$  values reported by Schrauzer and Holland in 1971 (592 nm in benzene, 614 nm in  $\text{CH}_3\text{OH}$ ) are thus closer to those obtained for the Co(I) compound of identical stoichiometry and charge is  $[\text{Co}(\text{dmgH})(\text{dmgH}_2)(\text{PnBu}_3)]$ , with a protonated glyoximate bridge.<sup>1</sup> By contrast with anionic **3**, this neutral species is expected to be highly soluble in nonpolar solvents such as *n*-hexane. In fact, the compound described by Schrauzer can also be formed by careful acidification of alkaline solutions of  $[\text{Co}(\text{dmgH})_2(\text{PnBu}_3)]^-$ , which further strengthens the relevance of considering the possibility of bridge protonation.<sup>19</sup> As a test, we optimized the structure of  $[\text{Co}(\text{dmgH})(\text{dmgH}_2)(\text{PnBu}_3)]$  at the BP86/TZVP level of theory (see Figure 6 and Supporting Information, Table S9) and found it to be only 12 kJ/mol less stable than the hydridocobaloxime **2**. We also calculated the NMR shifts in the same way as for **2**. The chemical shift for the  $\text{dmgH}_2$  proton that points outward from

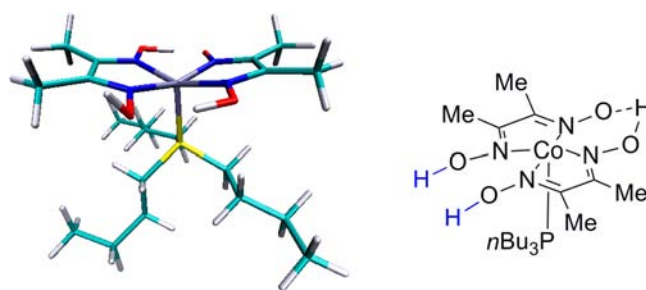


**Figure 6.** Geometry-optimized structure of the bridge-protonated  $[\text{Co}(\text{dmgH})(\text{dmgH}_2)(\text{PnBu}_3)]$  isomer of **2** in acetonitrile using the BP86 functional and the TZVP basis set.

the bridge, as shown in Figure 6, was found to be 6.5 ppm, which is close to the value that Schrauzer et al. observed. In addition, TDDFT/BP86 calculations of this compound produced several absorption bands in the region of 500 to 600 nm (see Supporting Information, Tables S10 and S11). These results are suggestive, but we refrain from making any concluding remark about this possibility without further experimental support and because we were not able to find the experimental conditions that gave a compound with spectroscopic features similar to those reported in the initial communication from 1971.<sup>18</sup>

## CONCLUSION

In this paper, we have characterized, using a combination of theoretical and experimental approaches, the hydrido-cobaloxime  $[\text{HCo}(\text{dmgH})_2(\text{PnBu}_3)]$  complex, which is thought to be a model of the hydride intermediate involved in hydrogen evolution catalyzed by cobaloxime<sup>4–9,12–15</sup> and cobalt diimine-dioxime<sup>3,4</sup> compounds. Such a complex was first described by Schrauzer et al. in the 1970s,<sup>18</sup> although there were some anomalies in the spectroscopic data that were reported there. In this work, we show that  $[\text{HCo}(\text{dmgH})_2(\text{PnBu}_3)]$ , with a clear hydridic nature and a bluish-purple color, can indeed be prepared following the procedure described by Schrauzer et al. but that these authors likely obtained and characterized another

compound. One possibility for this is an isomeric bridge-protonated cobalt(I) species, which raises interesting perspectives concerning the role of such alternative protonation sites in cobaloxime-catalyzed H<sub>2</sub> evolution.

## ■ ASSOCIATED CONTENT

### ■ Supporting Information

Further details are given in Figures S1–S8 and Tables S1–S11. This material is available free of charge via the Internet at <http://pubs.acs.org>.

## ■ AUTHOR INFORMATION

### Corresponding Author

\*Fax: 0033 438785494 (M.J.F.), 0033 438789124 (V.A.). Phone: 0033 438789594 (M.J.F.), 0033 438789106 (V.A.). E-mail: [martin.field@ibs.fr](mailto:martin.field@ibs.fr) (M.J.F.), [vincent.artero@cea.fr](mailto:vincent.artero@cea.fr) (V.A.).

### Notes

The authors declare no competing financial interest.

## ■ ACKNOWLEDGMENTS

Financial support from the French National Research Agency (ANR, NiFe-Cat ANR-10-BLAN-711) and the FP7 CEA-Eurotalents COFUND Program are gratefully acknowledged.

## ■ REFERENCES

- (1) Chao, T. H.; Espenson, J. H. *J. Am. Chem. Soc.* **1978**, *100*, 129–133.
- (2) Dempsey, J. L.; Brunswig, B. S.; Winkler, J. R.; Gray, H. B. *Acc. Chem. Res.* **2009**, *42*, 1995–2004.
- (3) Jacques, P.-A.; Artero, V.; Pécaut, J.; Fontecave, M. *Proc. Natl. Acad. Sci. U.S.A.* **2009**, *106*, 20627–20632.
- (4) Artero, V.; Chavarot-Kerlidou, M.; Fontecave, M. *Angew. Chem., Int. Ed.* **2011**, *50*, 7238–7266.
- (5) Razavet, M.; Artero, V.; Fontecave, M. *Inorg. Chem.* **2005**, *44*, 4786–4795.
- (6) Baffert, C.; Artero, V.; Fontecave, M. *Inorg. Chem.* **2007**, *46*, 1817–1824.
- (7) Hu, X. L.; Cossairt, B. M.; Brunswig, B. S.; Lewis, N. S.; Peters, J. C. *Chem. Commun.* **2005**, 4723–4725.
- (8) Hu, X.; Brunswig, B. S.; Peters, J. C. *J. Am. Chem. Soc.* **2007**, *129*, 8988–8998.
- (9) Pantani, O.; Anxolabehere-Mallart, E.; Aukauloo, A.; Millet, P. *Electrochem. Commun.* **2007**, *9*, 54–58.
- (10) Dempsey, J. L.; Winkler, J. R.; Gray, H. B. *J. Am. Chem. Soc.* **2010**, *132*, 1060–1065.
- (11) Dempsey, J. L.; Winkler, J. R.; Gray, H. B. *J. Am. Chem. Soc.* **2010**, *132*, 16774–16776.
- (12) Du, P. W.; Schneider, J.; Luo, G. G.; Brennessel, W. W.; Eisenberg, R. *Inorg. Chem.* **2009**, *48*, 4952–4962.
- (13) Du, P. W.; Knowles, K.; Eisenberg, R. *J. Am. Chem. Soc.* **2008**, *130*, 12576–12577.
- (14) Lazarides, T.; McCormick, T.; Du, P. W.; Luo, G. G.; Lindley, B.; Eisenberg, R. *J. Am. Chem. Soc.* **2009**, *131*, 9192–9194.
- (15) McCormick, T. M.; Calitree, B. D.; Orchard, A.; Kraut, N. D.; Bright, F. V.; Detty, M. R.; Eisenberg, R. *J. Am. Chem. Soc.* **2010**, *132*, 15480–15483.
- (16) Muckerman, J. T.; Fujita, E. *Chem Commun* **2011**, *47*, 12456–12458.
- (17) Solis, B. H.; Hammes-Schiffer, S. *Inorg. Chem.* **2011**, *47*, 11252–11262.
- (18) Schrauzer, G. N.; Holland, R. J. *J. Am. Chem. Soc.* **1971**, *93*, 1505–1506.
- (19) Schrauzer, G. N.; Windgassen, R. J.; Kohnle, J. *Chem. Ber. Recl.* **1965**, *98*, 3324–3333.

- (20) Caffyn, A. J. M.; Feng, S. G.; Dierdorf, A.; Gamble, A. S.; Eldredge, P. A.; Vossen, M. R.; White, P. S.; Templeton, J. L. *Organometallics* **1991**, *10*, 2842–2848.
- (21) Figueroa, J. S.; Cummins, C. C. *J. Am. Chem. Soc.* **2003**, *125*, 4020–4021.
- (22) Haller, L. J. L.; Mas-Marza, E.; Moreno, A.; Lowe, J. P.; Macgregor, S. A.; Mahon, M. F.; Pregosin, P. S.; Whittlesey, M. K. *J. Am. Chem. Soc.* **2009**, *131*, 9618–9619.
- (23) Kaesz, H. D.; Saillant, R. B. *Chem. Rev.* **1972**, *72*, 231–281.
- (24) Ruiz-Morales, Y.; Schreckenbach, G.; Ziegler, T. *Organometallics* **1996**, *15*, 3920–3923.
- (25) del Rosal, I.; Maron, L.; Poteau, R.; Jolibois, F. *Dalton Trans.* **2008**, 3959–3970.
- (26) Rahman, A. F. M.; Jackson, W. G.; Willis, A. C.; Rae, A. D. *Chem Commun* **2003**, 2748–2749.
- (27) Szajna-Fuller, E.; Bakac, A. *Eur. J. Inorg. Chem.* **2010**, 2488–2494.
- (28) Schrauzer, G. N. *Inorg. Synth.* **1968**, *11*, 61.
- (29) Toscano, P. J.; Swider, T. F.; Marzilli, L. G.; Brescianipahor, N.; Randaccio, L. *Inorg. Chem.* **1983**, *22*, 3416–3421.
- (30) Costa, G.; Mestroni, G.; de Savognani, E. *Inorg. Chim. Acta* **1969**, *3*, 323–328.
- (31) Weakley, T. J. R.; Marks, J.; Finke, R. G. *Acta Crystallogr., Sect. C: Cryst. Struct. Commun.* **1994**, *50*, 1690–1692.
- (32) Neese, F. *The Orca Program System. WIREs: Comput. Mol. Sci.* **2012**, DOI: 10.1002/wcms.81.
- (33) Becke, A. D. *Phys. Rev. A* **1988**, *38*, 3098–3100.
- (34) Lee, C.; Yang, W.; Parr, R. G. *Phys. Rev. B* **1988**, *37*, 785–789.
- (35) Becke, A. D. *Chem. Phys.* **1993**, *98*, 5648–5652.
- (36) Perdew, J. P. *Phys. Rev. B* **1986**, *33*, 8822–8824.
- (37) Kornobis, K.; Kumar, N.; Wong, B. M.; Lodowski, P.; Jaworska, M.; Andruniów, T.; Ruud, K.; Kozłowski, P. M. *J. Phys. Chem. A* **2011**, *115*, 1280–1292.
- (38) Andruniów, T.; Jaworska, M.; Lodowski, P.; Zgierski, M.; Dreos, R.; Randaccio, T.; Ruud, K.; Kozłowski, P. M. *J. Chem. Phys.* **2009**, *131*, 105105.
- (39) Grimme, S. *J. Chem. Phys.* **2003**, *118*, 9095–9102.
- (40) Weigend, F.; Ahlrichs, R. *Phys. Chem. Chem. Phys.* **2005**, *7*, 3297–3305.
- (41) Hrobarik, P.; Hrobarikova, V.; Meier, F.; Repisky, M.; Komorovsky, S.; Kaupp, M. *J. Phys. Chem. A* **2011**, *115*, 5654–5659.
- (42) Mulliken, R. S. *J. Chem. Phys.* **1955**, *23*, 1833–1840.
- (43) Mulliken, R. S. *J. Chem. Phys.* **1955**, *23*, 1841–1846.
- (44) Kutzelnigg, W.; Fleischer, U.; Schindler, M. *NMR Basic Principles and Progress* **1991**, *23*, 165–262.
- (45) Kutzelnigg, W.; Fleischer, U.; Schindler, M. *The IGLO-Method: Ab Initio Calculation and Interpretation of NMR Chemical Shifts and Magnetic Susceptibilities*; Springer-Verlag: Heidelberg, Germany, 1990; Vol. 23.
- (46) Bresciani-Pahor, N.; Calligaris, M.; Randaccio, L. *Inorg. Chim. Acta* **1980**, *39*, 173–179.
- (47) Coe, B. J.; Glenwright, S. J. *Coord. Chem. Rev.* **2000**, *203*, 5–80.
- (48) Kaesz, H.; Saillant, R. *Chem. Rev.* **1972**, *72*, 231–281.
- (49) Mock, M. T.; Potter, R. G.; O'Hagan, M. J.; Camaioni, D. M.; Dougherty, W. G.; Kassel, W. S.; DuBois, D. L. *Inorg. Chem.* **2011**, *50*, 11914–11928.
- (50) Bill, E.; Bothe, E.; Chaudhuri, P.; Chlopek, K.; Herebian, D.; Kokatam, S.; Ray, K.; Weyhermüller, T.; Neese, F.; Wieghardt, K. *Chem.—Eur. J.* **2005**, *11*, 204–224.
- (51) Nguyen, M. T. D.; Charlot, M.-F.; Aukauloo, A. *J. Phys. Chem. A* **2011**, *115*, 911–922.